Revista Mexicana de Ingeniería Química

Vol. 11, No. 2 (2012) 193-210

OPTICAL, MICROSTRUCTURAL, FUNCTIONAL AND NANOMECHANICAL PROPERTIES OF *Aloe vera* GEL/GELLAN GUM EDIBLE FILMS

PROPIEDADES ÓPTICAS, MICROESTRUCTURALES, FUNCIONALES Y NANOMECÁNICAS DE PELÍCULAS COMESTIBLES DE GEL DE *Aloe vera*/GOMA GELANO

J.S. Alvarado-González[1], J.J. Chanona-Pérez[1*], J. S. Welti-Chanes[2], G. Calderón-Domínguez[1], I. Arzate-Vázquez[3], S. U. Pacheco-Alcalá[4], V. Garibay-Febles[4] and G. F. Gutiérrez-López[1]

[1]*Departamento de Ingeniería Bioquímica, Escuela Nacional de Ciencias Biológicas, Instituto Politécnico Nacional, Plan de Ayala y Carpio s/n, Col. Santo Tomás, C.P. 11340, México, D.F.*

[2]*División de Biotecnología y Alimentos, Instituto Tecnológico y de Estudios Superiores de Monterrey, Av. Eugenio Garza Sada 2501 Sur, Col. Tecnológico, Monterrey, NL 64849, México*

[3]*Centro de Nanociencias y Micro y Nanotecnologías, Instituto Politécnico Nacional, Luis Enrique Erro s/n, Unidad Profesional Adolfo López Mateos, Col. Zacatenco, C.P. 07738, México, D.F.*

[4]*Laboratorio de Microscopía de Ultra Alta Resolución, Instituto Mexicano del Petróleo, Eje Central Lázaro Cárdenas 152, Col. San Bartolo Atepehuacan, C.P. 07730, México*

Received 30 of April 2012; Accepted 25 of June 2012

Abstract

Edible films of *Aloe vera* gel (Al), gellan gum (Ge) and their blend (AlGe) were prepared by the casting method and dried in a conventional oven. Optical, microstructural, functional and nanomechanical properties were evaluated. The films elaborated had adequate optical properties to be used in foods; AlGe showed higher values of transparency (6.5), total color difference (5.4) and extinction coefficient (0.052) than the Al and Ge; however, intermediate gloss (34.4) and refractive index (1.53) values were obtained for AlGe, maybe promoted by chemical interactions between *Aloe vera* and gellan gum. Microscopy and image analysis techniques were used to evaluate the microstructure of pure and blend films; the interactions due to the crosslinked among the polysaccharides of the blend were elucidated by atomic force microscopy. Water sorption capacity (-0.42 %/min) and water vapor permeability (21.3 g·mm/d·m^2·kPa) of AlGe were enhanced as compared to Al and Ge; besides the hardness (2.3 MPa) and elastic modulus (0.1 GPa) of the blend at nanometric level was reinforced with the gellan gum addition. The present research could be helpful to understand the blending effect on the property-structure-functionality relationships of edible films with potential use in food industry.

Keywords: edible films, *Aloe vera*, gellan gum.

Resumen

Se prepararon películas comestibles de gel de *Aloe vera* (Al), goma gelana (Ge) y su mezcla (AlGe), se utilizó el método de vaciado y se secaron en un horno convencional. Se evaluaron la propiedades ópticas, microestructurales, funcionales y nanomecánicas. Las películas elaboradas tuvieron propiedades ópticas adecuadas para su uso en alimentos; AlGe mostró altos valores de transparencia (6.5), diferencia total de color (5.4) y coeficiente de extinción (0.052) en comparación con la Al y Ge. Sin embargo, se obtuvieron valores intermedios de brillo (34.4) e índice de refracción (1.53) para AlGe; debido a las interacciones químicas entre *Aloe vera* y la goma gelano. Las técnicas de microscopía y el análisis de imágenes se usaron para evaluar la microestructura de películas puras y en mezcla; las interacciones debido al entrecruzamiento entre polisacáridos se elucidaron por medio del microscopio de fuerza atómica. La capacidad de absorción de agua (-0.42 %/min) y la permeabilidad al vapor de agua (21.3 g·mm/d·m^2·kPa) de la AlGe se mejoraron con respecto a la Al y la Ge. Así como, a nivel nanométrico, la dureza (2.3 MPa) y el módulo elástico (0.1 GPa) de la mezcla se reforzó con la adición de goma gelano. La presente investigación podría ser de ayuda para entender el efecto del mezclado en las relaciones propiedad-estructura-funcionalidad de películas comestibles con potencial uso en la industria alimentaria.

Palabras clave: películas comestibles, *Aloe vera*, goma gelano.

[*]*Corresponding author. E-mail*: jorge_chanona@hotmail.com

1 Introduction

The global market of *Aloe* primary products is valued around the 65 million dollars and more than 200 thousand million dollars in final products, such as lotions, beverages and medical supplies (Piña and Morales, 2010). *Aloe* gel is located in a zone between the abaxial and adaxial mesophile of *Aloe vera* plant. It is a viscous liquid inside the cells and organelles of parenchyma tissue (Domínguez-Fernández *et al*., 2012). The gel contains 95.4% water and 4.6% of total solids, which 60 % of that total solids are mucilaginous polysaccharides, mainly glucomannan that is responsible of some functional properties of the Aloe such as cohesivity, swelling, water retention capacity, fat adsorption capacity, gelation capacity, among other (Rodríguez-González *et al*., 2012; Sittikijyothin *et al*., 2005).

Aloe gel is also used as an edible cover as it has been applied to fruits to retard color changes, weight loss and softening. In some cases *Aloe* gel allows to keep high levels of total antioxidants and ascorbic acid in covered food products (Castillo *et al*., 2010). Alternatively, the biopolymers are used to create edible films that are applied as barriers to preserve and delay food deterioration. Recently researchers have been dedicated to create edible films that improve the food properties such as color, texture, flavor and overall appearance (Abugoch *et al*., 2011; Bergo *et al*., 2010). However, *Aloe* gel films have high water permeability and some barrier lacks. Therefore, mixtures with some compounds (cellulose, gelatin, etc.) have been studied in order to improve water and gases diffusion of films (Saibuatong and Phisalaphong, 2010).

Gellan gum is also a well-known biopolymer for its functional characteristics such as high hardness and transparency, low water vapor permeability and smooth surfaces. Chemical structure of gellan is formed by repeated units of tetrasaccharides and the addition of very small quantities (around 0.5% w/v) to films enhances mechanical and barrier properties; mainly in presence of mannans where it creates a highly organized structure and compacted network of biopolymers (Miyoshi, 2007).

Furthermore, to design and create functional edible films from pure components and blends, it is necessary to evaluate optical, physical, mechanical and microstructural properties in order to associate with the functionality and structure of edible films (Miranda *et al*., 2010). Thus, Mu *et al*. (2012), Zhang and Zhang (2012) and Porter and Felton (2010) describe a series of experimental techniques to determine physical, mechanical, adhesive, thermal and permeability properties on the edible films. On the other hand, the nanoindenter is a novel tool in the biological area, used usually in materials science to evaluate film-coated products (Wei and Lin, 2005). Porter and Felton (2010) used a nanoindenter as an alternative to assess elastic modulus and hardness, the gloss determination using the glossmeter and the permeability by the cup method and concluded that those techniques allow the complete optimization and design of edible films.

The selection criteria for edible films are mostly based on their barrier and mechanical properties, especially in water vapor permeability (WVP) and elastic modulus (Romero-Bastida *et al*., 2011; Kechichian *et al*., 2010; Yener *et al*., 2009). The edible films that show the lowest values of WVP are selected as adequate films to apply in food industry and the elastic modulus also is considered as an important property of films (Villagómez-Zavala *et al*., 2008; Ayranci and Tunc *et al*., 2003). On the other hand; optical and microstructural properties have been relatively less reported in scientific literature, however the determination of those properties is equally important and in some research studies is critical for the final analysis of functional characteristics of edible films (Liu *et al*., 2012; Abugoch *et al*., 2011). For this reason, the aim of this work was to evaluate the optical, microstructural, and nanomechanical properties of *Aloe vera* gel/gellan gum edible films to understand the interactions and influence of the components on the functionally of pure and blend films.

2 Materials and methods

2.1 Procedure of films formation

Aloe vera gel (*Aloe* Jaumave SA de CV, México) with 3.3 % total solids content, as measured by refractometric method at 20°C (Abbe refactometer, Ermal optical Works, Japan), and gellan gum powder (catalog number: G1910) were used to made the edible films. Gellan gum was selected as support component to prepared edible films due to improvement of optical, barrier and mechanical properties (Tapia *et al*., 2008; Lau *et al*., 2001), such as transparency, water vapor permeability and high tensile strength (Tang, 1998; Pranoto *et al*., 2007; Lee *et al*., 2004). Glycerol (catalog number: G9012) was employed as plasticizer to obtain freestanding *Aloe vera* and blend films.

Gellan gum and glycerol were analytic grade and were provided by Sigma-Aldrich (USA).

Aloe vera solution were heated at 60 °C and then added with 1% v/v of glycerol while agitating with a magnetic stirrer (Barnstead International, USA) for 15 minutes. Gellan gum solution (0.5% w/v) was prepared with distilled water preheated at 90 °C, without glycerol and stirred until total homogenization (30 minutes) with the same magnetic stirrer aforementioned. Blend solution was formed by a mixture of *Aloe vera* and gellan gum solutions at a volume ratio of 1:1 and stirred for 25 minutes. Films formulation were chosen based on several reports about elaboration of edible films (Banerjee and Bhattacharya, 2011; Carneiro-da-Cunha *et al*., 2010; Chen *et al*., 2010; Lau *et al*., 2001, Lee *et al*., 2004) and the volume ratio of blend films was selected in order to evaluate a formulation with a similar proportion of components. In contrast with Aloe films, the gellan films could be obtained without glycerol addition, because they were freestanding films and easily removable from container where these films were formed. Fifteen grams of edible films solutions were poured into glass Petri dishes of 60 × 15 mm (Pyrex, USA) and for film formation the solutions were dried in an oven (Shel Lab GI6, USA) at 60 °C until constant weight, according by Ramachandra and Srinivasa Rao, (2008). After drying, the formed films were placed in an automatic desiccator (Bel-Art Products 420721115, USA) at ambient temperature and 15% relative humidity (RH) which according to Ramachandra and Srivinasa (2009) is the RH value appropriate for moisture homogenization of film samples; after 24 hours the samples were removed from the desiccator and then analyzed. Thus, three films were prepared and named as follow, Al (*Aloe vera* film), Ge (gellan gum film) and the blend of AlGe (*Aloe vera*/gellan gum film).

2.2 Optical properties

2.2.1. Transparency

Film transparency was estimated by using modified ASTM D1746-97 (ASTM, 2000c) method and according the procedure reported by Nadarajah (2005) with a spectrophotometer (Genesys 10-S, Thermo Fischer Scientific, USA). Film samples were cut into rectangular shapes and placed on the interior of the spectrophotometer cell. Transparency was calculated with the equation proposed by Hans and Floros (1997):

$$Tp = \frac{A_{600}}{b} \tag{1}$$

where A_{600} is the absorbance at 600 nm and b is the thickness of the film (nm). Thickness was measured with an automatic micrometer (Fowler, IP54, China) with 0.2 μm of accuracy.

2.2.2. Color

Color parameters in CIELab color space were directly estimated with CR-400 colorimeter (Konica-Minolta, Sensing Inc., USA) with D65 light source, 0° and aperture diameter of 8 mm. Films samples (50 mm × 25 mm) were placed on a white standard plate (white calibration standard plate 19633130) and read to obtain the spectra data. Total color difference (ΔE) was calculated with the equation described by Monedero *et al*. (2008):

$$\Delta E = \sqrt{(\Delta L^*)^2 + (\Delta a^*)^2 + (\Delta b^*)^2}$$

where $\Delta L^* = L^* - L_0^*$, $\Delta a^* = a^* - a_0^*$, $\Delta b^* = b^* - b_0^*$, being L_0^*, a_0^*, b_0^* the color parameter values of white standard plate and L^*, a^*, b^* the color parameter values of the film samples.

2.2.3. Refractive index and extinction coefficient

An ellipsometer (UVISEL LT M200 AGMS, Yvon Horiba, France) was used to determined the refractive index (n) and extinction coefficient (k) of edible films according to the method reported by Murray and Dutcher (2006) and Nosal *et al*. (2005). The spectral range applied was 450 nm to 650 nm with an angle of incidence of 70° in three different areas selected randomly.

2.2.4. Gloss

The gloss parameter of the edible films was measured with a glossmeter (MG268-F2, KSJ, China) according the norm ASTM D523 (1999) and the method described by Villalobos *et al*. (2005). The films were cut (75 mm x 25 mm) and placed onto the black glass standard (Serial number F21010611) and read directly on the film surface at different incidence angles (20°, 60° and 85°). Results were expressed as gloss units (GU) referring to the black glass standard with a value approximately of 100 gloss units.

2.3 Microscopy studies

2.3.1. Light microscopy (LM) and image analysis

The microstructure surfaces of the edible films were visualized in a light microscope (Nikon Eclipse 50i, Japan). Film cuts of 2.5x2.5 cm were placed on a microscope slide and observed at 10x magnification at five different zones randomly. Images were captured with a CCD camera (Nikon DS-2Mv, Japan) and saved in RGB color and TIFF format by using the Nis Elements software (F2.30, Nikon, Japan). The acquisition conditions of images were always the same for all samples (exposure time: 1/1000 s, gain of 1.0 and contrast in enhanced mode).

Texture image analysis was applied to quantitatively characterize the surface microstructure of edible films. The image texture is a characteristic representing the spatial arrangement of the gray levels of pixels of the image (Arzate-Vázquez *et al*., 2012). In this work two texture features were selected as parameters of study (Homogeneity: Hm and Entropy: En). Homogeneity, also called inverse difference moment is a measure of the local homogeneity of the image, higher values can be associated to smooth surfaces. Entropy measures the disorder or randomness of images, and can be used to characterize the image texture. It is an indication of the complexity within an image, so the more complex images, the higher entropy values. Thus, the images obtained from light microscopy were converted from RBG color to gray-scale images; subsequently, Gray Level Co-Ocurrence Matrix (GLCM) algorithms were applied to obtain texture features from gray scale images (Haralick *et al*., 1973). According to Haralick *et al*. (1973), with the GLCM algorithm is possible to calculate fourteen texture parameters. However, we only considered useful: homogeneity and entropy as the other parameters could be redundant as reported recently (Mendoza *et al*., 2007; Meraz-Torres *et al*., 2011; Arzate-Vázquez *et al*., 2012). The whole image analysis methodology was carried out using the software ImageJ v 1.34s (National Institutes Health, Bethesda, MD, USA). Thus, entropy measures the disorder or randomness of gray scale images and homogeneity is the measure of local variations of gray level values of images pixels (Yang *et al*., 2000; Arzate-Vázquez *et al*., 2012).

2.3.2. Environmental scanning electronic microscopy (ESEM)

ESEM system (XL 30, Philips, USA) was employed to visualize the overall morphology of film surfaces. This microscopy allows the essays of wet biological materials without previous preparation (Arzate-Vázquez *et al*., 2012). Thus, films of 4 mm x 4 mm were fixed on the sample holder with double-sided carbon tape, without metallic conductive cover, and observed under ESEM system. Micrographs were captured at 300x magnification in gray-scale using a voltage of 25 kV and finally stored at TIFF format in similar conditions reported by Quintanilla-Carvajal *et al*. (2011).

2.3.3. Atomic force microscopy (AFM)

AFM allows the analysis of the surface topography at nanometric levels and makes possible the creation of 3D models showing in minor detail the microstructure of the sample such as interaction and arrangement of polymeric components. AFM (Multimode IV NanoScope, Veeco, USA) in tapping mode were applied to the films using SiN_4 tip (Yang *et al*., 2007). Scanning area was $1\mu m \times 1\mu m$ and the micrographs were analyzed for surface roughness (Ra) with the software NanoScope v 7.30 (Veeco, USA). Ra values and 3D surfaces were obtained from the height images.

2.4 Functional properties

2.4.1. Water sorption capacity

Water sorption capacity (WSC) of films was evaluated by weighing and soaking the samples for 30 minutes in phosphate buffered saline solution (PBS, pH 7.4) at room temperature according to the methodology proposed by Nadarajah (2005). After soaking time, the films were removed from the PBS solution and the excess was gently wiped off from the surface of the film with a piece of filter paper and immediately weighed. The percent of water sorption capacity (%) of films was calculated from to the equation reported by Çaykara and Turan (2006):

$$WSC = \frac{W_S - W_D}{W_D} * 100$$

where, W_S is the weight of the swollen film after 30 minutes and W_D is the weight of the dried film.

2.4.2 Water vapor permeability

Water vapor permeability (WVP) was obtained from a variant of the ASTM, E 96-80 (1989) gravimetric method (permeability cup). The experimental units employed in this determination were reproduced with some modifications from the method proposed by Bosquez-Molina *et al*. (2003). These authors defined the WVP in terms of the differences of the specific partial pressure and relative humidity of the saturated solutions, the stagnant air, the measures of height and wide of the desiccator and as well as permeability cups dimensions.

Metallic permeability cups (MPC) were used to determine the WVP edible films. The MPC (13-338, Fisher/Payne, USA) height ranks of 1.2 cm and cross section area of 10.5 cm^2. A desiccator with flat top and a total height of 16 cm and diameter of 25.2 cm was used in the experiments. The distance between the MPC and the flat top of the desiccator was 11.3 cm.

A saturated KNO_3 solution with a relative humidity of 93 % was used as the inner solution of the MPC and a NaCl solution with relative humidity of 75 % was poured in the lower part of the desiccator. The MPC was filled with the KNO3 solution until reaching 0.6 cm of the vessel height and an edible film with a known weight was mounted on the upper side of the MPC. Once the edible film was set up, the MPC-sample system was weighed and put into the desiccator. The MPC-sample system was weighed every hour until reaching constant weight. The water vapor transmission rate (WVTR) was the first data acquired, a regression analysis were performed in terms of the modified formula reported by Wang *et al*. (2011):

$$WVTR = \frac{W_S}{ta} \tag{2}$$

where in Eq. (1) is water vapor transmission rate, W_S is the weight loss of the sample, t represents the treatment time and a is the cross section area exposed of the film.

Once the WVTR was calculated, the WVP was corrected by means of the methodologies reported by Gennadios *et al*. (1994) and Bosquez-Molina *et al*. (2003):

$$WVTR_C = WVRT_M\left(\frac{P_{KNO_3} - P_{Over}}{P_{NaCl} - P_{Under}}\right) \tag{3}$$

$$WVP_M = \left(\frac{WVRT_M x}{P_{KNO_3} - P_{Over}}\right) \tag{4}$$

$$WVP_C = \left(\frac{WVRT_C x}{P_{NaCl} - P_{Under}}\right) \tag{5}$$

where in Eq. (2) $WVTRc$ and $WVTR_M$ are the corrected and measured water vapor transmission rate, respectively. In Eqs. (3) and (4) WVP_C and WVP_M are the corrected and measured water vapor permeability, respectively. While, P_{KNO_3} and P_{NaCl} are the partial pressures of the saturated solutions; P_{Over} and P_{Under} are the partial pressures of the films on the surface and underside the film, respectively and x is the film thickness. The partial pressures P_{KNO_3}, P_{NaCl}, P_{Over} and P_{Under} were calculated with the geometrical data of the experimental unit correlating the distance of the MPC and the desiccator to the solutions of KNO_3 and NaCl according by Bosquez-Molina *et al*. (2003). The error percentage (% Error) was evaluated by using Eq. (5).

$$\%Error = \left(\frac{WVP_M - WVP_C}{WVP_C}\right) * 100 \tag{6}$$

2.5 Nanomechanical properties

Nanomechanical properties were characterized as Carneiro-da-Cunha *et al*., (2010) using a nanoindenter (Nanoindentation Tester NHT, CSM Instruments, Switzerland) which contains a Berkovich diamond tip to penetrate the sample and generate load-depth curves as is plotted in Fig. 1. The shape of the Berkovich indenter tip is a three-sided pyramid (Fig. 1). Oliver-Pharr method was used for calculated the nanomechanical properties (Fischer-Cripps, 2006). Sections of films were cut and mounted with glue on cover slips.

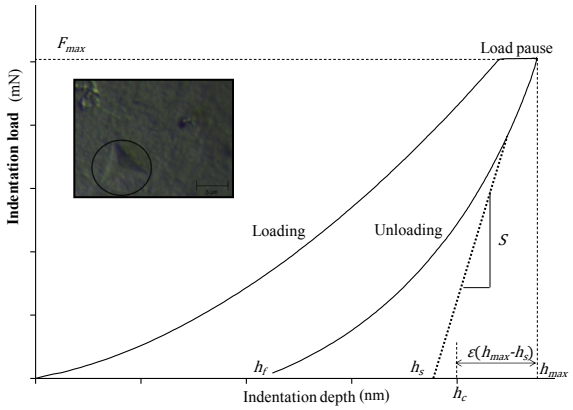

Fig. 1. Typical nanoindentation curve (Indentation load vs. indentation depth) and image of the three-sided pyramid mark produced by the Berkovich indenter in gellan gum film. See text for annotations.

Test variables used were: maximum load of 2.5 mN, loading and unloading rate of 7.5 mN/min and pause of 35 seconds. Before testing, the instrument was calibrated with a fused silica calibration standard.

Hardness (Hd) and elastic modulus (Em) values were obtained from acquired load-depth curves based on the geometric of the Berkovich indenter mark (Fig. 1). The following equations were used to obtain those nanomechanical parameters:

$$F = K\left(h - h_p\right)^m \tag{7}$$

$$h_c = h_{\max} - \varepsilon\left(h_{\max} - h_s\right) \tag{8}$$

$$A_p = C_0 h_c^2 + C_1 h_c + C_2 h_c^{1/2} + ... + C_8 h_c^{1/128} \tag{9}$$

where in Eq. (6); F is the force, h is the depth, h_p is the plastic depth and K and m are constants. The Eq. (7) describes the contact depth h_c, in terms of the depth h_s calculated from the intercept of the depth axis by the tangent line to the unloading curve and the ε constant value of 0.25 for Berkovich and Vickers indenters (Lucca *et al*., 2010). And finally, Eq. (8) were used to calculate "A_p" that refers to the projected area of contact of the indenter estimated in h_c, where the $C_0, ..., C_8$ are the machine compliance values in eight consecutive indentations upon a quartz piece of reference.

When the variables in Eqs. (6), (7) and (8) are calculated, the hardness and the elastic modulus can finally be estimated with the Krumova *et al*. (2002) and Oliver and Pharr (2004) equations. For the hardness:

$$Hd = \frac{F_{\max}}{A_p} \tag{10}$$

Where in Eq. (9) Hd is the hardness, F_{max} the maximum test force and A_p is described in Eq. (8). The elastic modulus is given by the two successive equations:

$$E_r = \frac{S\sqrt{\pi}}{2\sqrt{A_p}} \tag{11}$$

$$Em = \frac{(1 - v^2)}{\frac{1}{E_r} - \frac{(1-v_i^2)}{E_i}} \tag{12}$$

where E_r is the reduced modulus, S is the initial unloading stiffness in the load-depth curve and A_p from the Eq. (8). When Eq. (10) is solved, the Em is finally estimated with the Eq. (11) where Em is the elastic modulus, v is the Poisson's ratio for polymeric samples estimated in 0.35 (Krumova *et al*., 2002) and v_i and E_i are the Poisson's ratio of 0.07 and elastic modulus of 1141 GPa of the indenter (Lavorgna *et al*., 2010), respectively. All calculus, hardness and elastic modulus were estimated by means of the nanoindenter software.

2.6 Statistical analysis

All the parameters were expressed as the mean value and its corresponding standard deviation. Three replicates were used in all experiments. One-way Analysis of Variance (one-way ANOVA) was applied to compare statistically the data; followed by a Tukey multiple comparison test (Montgomery, 1991) with software SigmaStat 3.5. Significant differences were considered when $P < 0.05$. The plots were generated using the SigmaPlot software version 10.0.

3 Results

3.1 Optical properties

In Table 1, values of transparency (Tp) at 600 nm of the films are shown. It is noticeable that, when films were opaque Tp values increased. Ge sample resulted the most transparent film (4.1) followed by Al (4.9) and AlGe (6.5). The AlGe had a higher transparency value, than the one for hydroxylpropyl methyl cellulose blend films (Tp values of around 2) as reported by Jutaporn *et al*., (2011). According with Mu *et al*., (2012) the addition of dialdehyde carboxymethyl cellulose in gelatin edible films decrease the transparency, this fact may be due to crosslinking of relatively long polysaccharides in the structure of films. In Fig. 2, a photograph of the three films is shown and by visual inspection is noticeable that Al presented an appearance more opaque and heterogonous than AlGe and Ge, while Ge was the most transparent and homogenous film in comparison with the other films and intermediate characteristics of transparency and homogeneity are also observed in AlGe.

Fig. 2. Films appearance, a) *Aloe vera* film (Al); b) *Aloe vera* /gellan gum blend (AlGe) and c) gellan gum film (Ge).

Table 1. Transparency (Tp), total color difference (ΔE), Hardness (Hd) and elastic modulus (Em) of films.

Film	Tp	ΔE	Hd (MPa)	Em (GPa)
AlGe	6.5±0.03 a	5.4±0.3 a	2.3±0.2 a	0.1 ± 0.03 a
Al	4.9±0.01 b	4.6±0.1 b	0.9±0.2 b	0.05±0.01 b
Ge	4.1±0.03 c	4.3±0.2 b	171.9±5.2 c	2.02 ± 0.02 c

Values (mean ± standard deviation, $n = 5$) in the same column with the same letters are not significantly different ($P > 0.05$). *Aloe vera* film (Al); *Aloe vera* /gellan gum blend (AlGe) and gellan gum film (Ge).

Tp results showed a similar tendency to ΔE values (Table 1). ΔE values of Al and Ge oscillated from 4.3 to 4.6 and it was not observed significant differences ($P > 0.05$). Previous works reported ΔE values close to 4.9 for *Aloe* gel layer dried with hot air (Femenia *et al*., 2003). In the case of AlGe, the ΔE value increased in comparison with Al and Ge, even though the ΔE value of AlGe corresponded to colorless films according with the ΔE values reported by Maria *et al*., (2008) for blends of gelatin and five different types of polyvinyl alcohol. This change can be associated to hydrogen bonds between the polysaccharides of blend (Alves *et al*., 2011).

Moreover, the Tp and ΔE values also can be related with the extinction coefficient (k), while k depends directly on the light absorption, consequently k could be correlated with the opacity. Thus, higher k values can be associated to high film opacity (Jung and Kim, 2008). The Fig. 3 shows the k-wavelength plot, where the k values for Ge remain invariants (from 0.037 to 0.036) trough spectrum range studied and the lowest values of k compared with the other films indicates the lowest value of opacity (Banerjee *et al*., 2011). Al was more opaque (from 0.041 to 0.045) than the Ge and consequently the k values increased, while AlGe was the most opaque film (from 0.047 to 0.052). These results suggest that the chemical interactions between gellan gum and *Aloe vera* could influence the optical properties in the blend film (Banerjee and Bhattacharya, 2011; Lau *et al*., 2001).

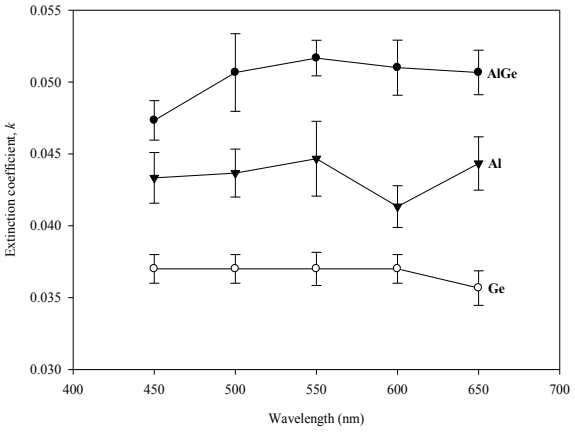

Fig. 3. Values of extinction coefficient (k) of films at different wavelength. *Aloe vera* film (Al); *Aloe vera* /gellan gum blend (AlGe) and gellan gum film (Ge). Each point is an average of 5 determinations and the error bars represent the standard deviation.

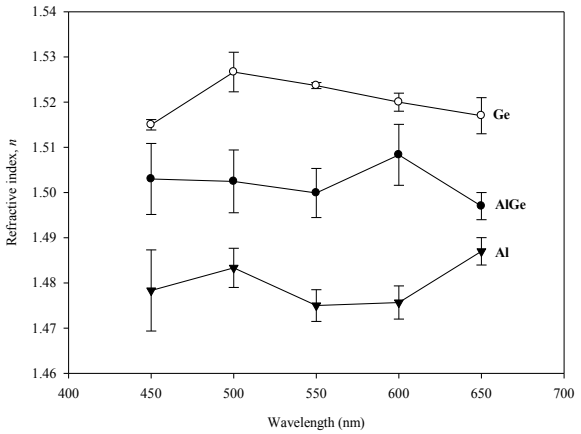

Fig. 4. Values of refractive index (n) of films at different wavelength. *Aloe vera* film (Al); *Aloe vera* /gellan gum blend (AlGe) and gellan gum film (Ge). Each point is an average of 5 determinations and the error bars represent the standard deviation.

Hence, Tp, ΔE, and k can be associated with the transmission and absorption of light; for this reason the AlGe showed a high opacity in comparison with Ge and Al. Thus, the high opacity of AlGe could be attributed to a major crosslinking between the mannans of *Aloe vera* and the tetrasaccharides units of gellan gum (Miyoshi, 2007).

Fig. 4 shows the refractive index (n) in function of wavelength, where n is the numerical representation of light propagation through a media and the resulting deflection is an important optical property in foods, especially in packing (Illiger *et al*., 2009); The n values showed a tendency to remain constant. Thus, the Ge showed the highest values of n (from1.52 to 1.53) due to the alignment of the polymeric chains, in comparison with the Al (from1.48 to 1.49) where the inner amorphous structure could be larger. On the contrary, the AlGe showed intermediate values of refractive index (from 1.50 to 1.53) due that to the blend could have a medium amorphous state (Liu *et al*., 2007). The n values obtained were similar to those reported by Jones (2010) for chitosan films (n = 1.5).

In the case of the gloss measurements (Fig. 5), the tendency was similar to the n values obtained. The glossiest film was the one elaborated with Ge, with very high values at all angles, especially at 60° (124 GU); this value was comparable to those obtained with films prepared with whey protein isolates, as they can reach 144 GU at 20° of light incidence (Lee *et al*., 2008). Gloss results depends on the illumination incidence angle, having been observed that medium values of gloss are effectively evaluated at 45°, while lower gloss values are better assessed when using higher angle values. This has been attributed to the enhancement of specular reflection when the incidence angle increases (Fabra *et al*., 2011), for this reason is necessary to evaluate the gloss at different angles. Therefore, the Al and AlGe did not show significant difference ($P > 0.05$) in gloss at 20° and 85° however at 60° is clear the separation of gloss values for films. As a result at 60°, the glossiest film was the one prepared with AlGe (34.4 GU) in comparison with Al (24.9 GU), where the gloss is improved in AlGe when the gum is added (Ward and Nussinovitch, 1997).

In overall, the optical properties (transparency, color, n, k and gloss) determined in the films, can be associated with their polymeric structure and chemical composition of the biopolymer used. For instance gellan gum have a alignment structure in long chains of tetrasaccharides that provide structural support and homogeneity to the films, while the mannans of *Aloe vera* provide a heterogonous and amorphous structure to the films. In the blend films these properties are combined and middle optical properties were observed in blend films; chemical interaction as hydrogen bonds and aldol condensation between carbonyl of the acetyl groups of mannans and carboxyl groups of tetrasaccharides could occur, promoted by blending and drying process. Thus, gellan gum provides transparency, gloss and structural support, while *Aloe vera* confers opacity, color and an amorphous structure to films when these components are blended.

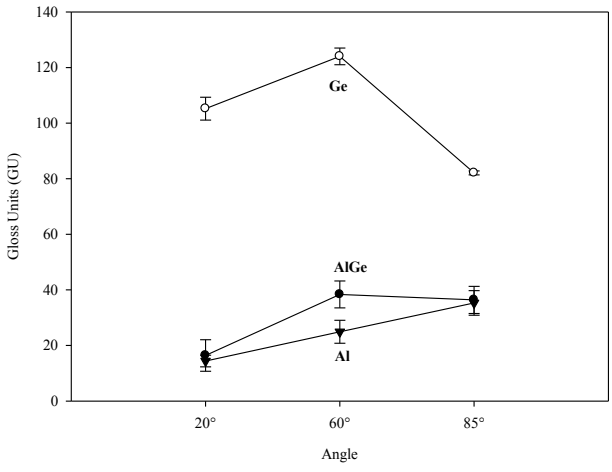

Fig. 5. Gloss units of films at 20°, 60° and 85° angles. *Aloe vera* film (Al); *Aloe vera* /gellan gum blend (AlGe) and gellan gum film (Ge). Each point is an average of 5 determinations and the error bars represent the standard deviation.

Consequently, light properties as transmission (k) and refraction (n) also was modified by structural and chemical interaction between the biopolymers used for elaboration of films.

3.2 Microscopy studies and image analysis

Fig. 6 shows LM and ESEM images of the films microstructure. In overall, Al presented the roughest structure followed by AlGe and Ge. In LM, the Al film showed rough surfaces associated to parts of cellular fibers, wall cell and cytoplasm (Domínguez-Fernández *et al*., 2012). While Ge presented the smoothest surface and homogenous microstructure, that can be attributed to the ordered arrangement of the tetrasaccharides in its polymeric chains (Dentini *et al*., 2001). AlGe showed a less rough surface than Al due to a minor content of cellular elements and also for the combination of the polymeric compounds of Al and Ge. To evaluate surface microstructure of the films image texture analysis provides parameters to measure homogeneity and disorder or complexity of images (Yang *et al*., 2000). Fig 6 shows the values of entropy (En) and homogeneity (Hm) for the LM images, these parameters express quantitatively the topography characteristics of the films micrographs. Consequently, Hm parameter indicates that Ge has the highest homogeneity (0.29), and the lowest entropy (6.87). With regard to Al, the En was high (9.24) in comparison with the other films, therefore the film is more heterogeneous with a Hm value of 0.07. While, AlGe showed intermediate values of En (8.13) and Hm (0.15), that can be attributed to the combination of the organized structure of gellan gum and amorphous arrangement of *Aloe vera*, which yields structuring in the AlGe. A previous work showed that the En and Hm were similar to chitosan, alginate and blend films (Arzate-Vázquez *et al*., 2012).

In ESEM images (Fig. 6), the films microstructure was similar to those observed in LM. In Al micrographs the surface is very heterogeneous and several fissures and cracks were observed; the heterogeneity composition of *Aloe vera* and the drying process could promote these irregularities. In opposite, the microstructure of Ge showed a homogenous surface and some fibrillar folding due to polymeric matrix of gellan gum. Finally, AlGe showed a surface with multiple fibrillar folding and branched forms apparently due to the drying process and the blending of the materials. Similar structures were found in a composite film of *Aloe vera*/cellulose, where the structure became more heterogeneous with abundant gel on the film surface (Saibuatong and Phisalaphong, 2010).

Images at major resolution were obtained by AFM; with this technique a small scan area (1μm x 1μm) can be studied. AFM resolve nanometric structures in the films (Fig. 7) and it allows observing some polymeric interactions (Fernández-Pan *et al*., 2010). The AFM images were evaluated by Ra parameter, this value was indicated at the top of each LM image (Fig. 4). Under AFM the Al exhibited a highly rough and non-uniform structure in comparison with the Ge, which is highly ordered and showed an aligned and homogeneous arrangement. Furthermore; the characteristic structure of Ge is probably induced by the interaction between its functional groups when the gelation is occurring in gellan solutions. The channeling pattern is especially noticeable in the 3D image in Ge (Funami *et al*., 2008). In addition, a very smooth surface is reflected in the Ra value (1.5 nm) which is small in comparison with other films, such as chitosan or alginate edible films (Arzate-Vázquez *et al*., 2012). A highly heterogeneous surface raises the average of Ra values for Al (26.4 nm) in comparison with that of Ge.

Regarding AlGe, it had a microstructure with complex arrangement and fibrillar elements, although it still contains a relative homogenous topography as compare to Al. AFM images at nanometric resolution suggested that the blended structure can be related to the linking of the constituents rather than the effect of the drying process, maybe associated to gel-forming by means of the direct interactions of the two polymers of the blend (Oakenfull, 1991). AlGe topography images provided a Ra value of 9 nm and fibrillar structures with an average wide of 30 nm. This fact suggests the presence of non-covalent connecting bridges and matrix polysaccharides with the mannan and tetrasaccharides molecules (Moreira and Filho, 2008). Also, it is possible that the drying process promote covalent bonds between biopolymers by means of aldol condensation.

Microstructural studies provide useful information to explain the changes in optical, functional and nanomechanical properties. LM observations can be associated to overall appearance of films and with the optical properties; the blend films showed a microstructure that combines the homogenous structure of gellan gum and amorphous arrangement of *Aloe vera*. In consequence the transparency, color and gloss are influenced by structural and chemical interactions between the biopolymers used.

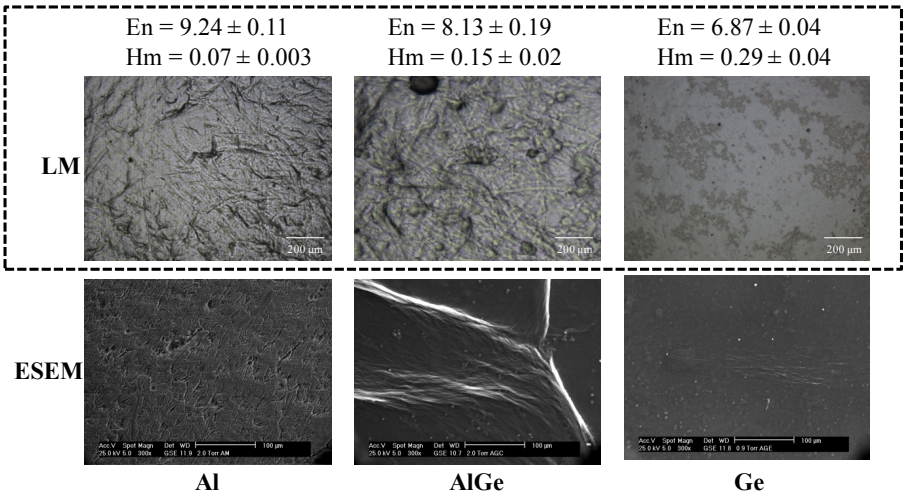

Fig. 6. Films micrographs obtained by LM (10x) and ESEM (300x). Square with dashed line corresponding to entropy (En) and homogeneity (Hm) values evaluated from LM images. *Aloe vera* film (Al); *Aloe vera* /gellan gum blend (AlGe) and gellan gum film (Ge).

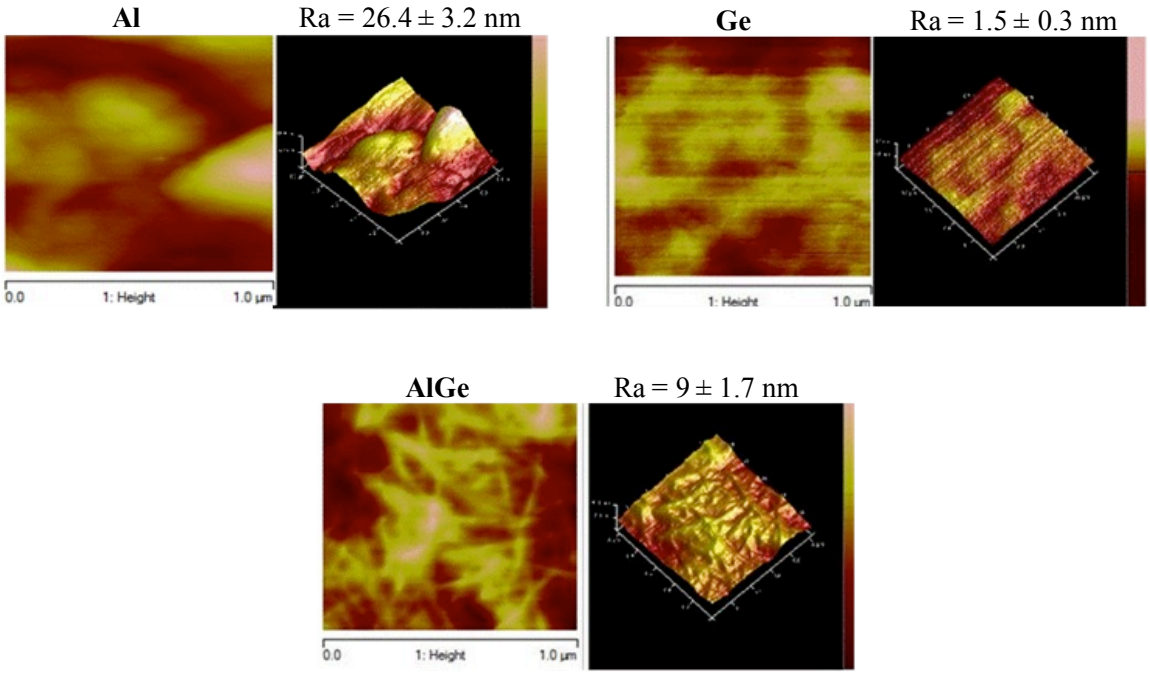

Fig. 7. AFM topographic images and 3D-topographic plots of films. Scan size (1 μm x 1 μm) and roughness values (Ra) are indicated. *Aloe vera* film (Al); *Aloe vera* /gellan gum blend (AlGe) and gellan gum film (Ge).

Also, the effects of drying process and the structural interaction between biopolymers were more evident in ESEM images. From AFM images, it is possible to observe the structural interaction of biopolymers in the blend; and a descriptive structural model can be proposed. Thus, the globular and amorphous matrix of *Aloe vera* was reinforced structurally by the aligned polysaccharides chains of the gellan gum, these promote an external and internal cross-linking in the blend films. Covalent and non-covalent chemical bonds could be responsible of the structural changes in AlGe films and the values obtained in optical,

functional and nanomechanical properties are affected as well by those bonds. The combined influence of the blended and the drying process could explain the changes on the functional and mechanical properties in the blend films. Their effects are described in following sections.

3.3 Functional properties

Water sorption capacity (WSC) as function of time for edible films is described in the Fig. 8, where Ge film showed positive WSC values, indicating a high capacity of water uptake, maybe due to swelling phenomenon. The Ge incremented WSC trough time, thus in 30 minutes WSC went from 0 % to 795 % and WSC rate was of around 23 %/min. The high WSC of Ge is associated to the arrangement of the gellan carbohydrate which develops a sponge like structure in the double helicoidal conformation of the gellan gum that allows the fast water uptake (Adachi, 2002; Dentini *et al*., 2001). Comparing with N-isopropylacrylamide hydrogel (Çaykara, 2004) and chitosan films (Nadarajah, 2005), the Ge displays low swelling values.

Regarding Al, negative WSC values were observed, probably due to the high film solubility, as it was rapidly dissolved into the buffer and the integrity of the film completely lost after 30 minutes. Thus, negative WSC values trough time and a WSC negative rate of -3.3 %/min were found for Al. It has been reported for mucilaginous materials and some edible films, that disintegration usually occurs when the sample is wetted, for instance okra gum is dissolved in 24 minutes (Ikoni and Obiageli, 2010), hibiscus mucilage in 90 minutes (Padmakumari *et al*., 2011), and films made from pullulan mucilage have the property to dissolve quickly, as a result freestanding pullulan films are used to fight halitosis (Barkalow *et al*., 2002).

Concerning AlGe, the WSC slightly diminished trough time, and when the AlGe is put into the buffer solution no swelling occurs. When the experiment time concluded, the AlGe appearance remained intact and an almost imperceptible raise was noticed on the film surface. For AlGe a decrement of 13 % in 30 minutes on WSC and a negative rate of -0.42 %/min were observed. This behavior can be explained from the interaction occurred between carbohydrates contained in the Aloe and gellan, which creates intricate networks that restrict the water absorption and provide partial impermeability to the film. This fact coincides with the cross-linked structure observed in the AFM micrographs. In other studies, carboxymethyl cellulose/gelatin blends presented a minimum swelling ratio of 151 % (Mu *et al*., 2012). Therefore, the AlGe provide interesting functional properties that could be attractive to cover food with high humidity.

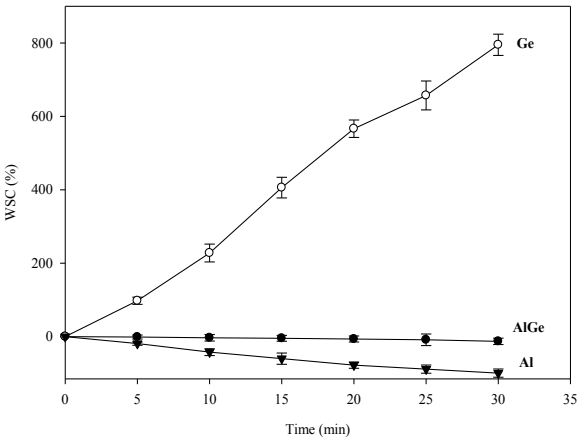

Fig. 8. Water sorption capacity (WSC) of films as a function of time. *Aloe vera* film (Al); *Aloe vera* /gellan gum blend (AlGe) and gellan gum film (Ge). Each point is an average of 5 determinations and the error bars represent the standard deviation.

Table 2. Thickness, water vapor permeability measured (WVP_M) and corrected (WVP_C) of films. Error percentage between WVP_M and WVP_C (Gennadios *et al*., 1994).

Film	Thickness (μm)	WVP_M (g·mm/d·m^2·Pa)	WVP_C (g·mm/d·m^2·Pa)	Error (%)
AlGe	58.3±2.2 a	25.2±3.6 a	21.3±3.5 a	15.2
Al	54.4±1.7 b	56.7±2.7 b	46.9±2.3 b	17.3
Ge	53.1±1.1 b	21.7±4.2 a	16.8±3.7 a	22.8

Values (mean ± standard deviation, $n = 5$) in the same column with the same letters are not significantly different ($P > 0.05$). *Aloe vera* film (Al); *Aloe vera* /gellan gum blend (AlGe) and gellan gum film (Ge).

The barrier properties of edible film, as WVP_c and thickness, help to determine their possible final application, which in many cases include covering high moisture foods (Rojas-Graü *et al*., 2008). Thus, WVP_c values and thickness of films are presented in Table 2, also can be observed that WVP_M showed high errors in a range of 15.2-22.8 % with respect to WVP_c. It is recommendable to report the corrected WVP values, because the classical methods overestimate the water vapor permeability as has been mentioned by Gennadios *et al*. (1994) and Bósquez-Molina *et al*. (2003). Thickness remained similar for the Al and Ge samples, oscillating from 53.1 to 54.4 μm and not significant differences were found ($P > 0.05$); However, AlGe was thicker (58.2 μm) than the other films ($P < 0.05$). The interaction between polymers and the drying process could have induced the thickening of the blend film (Ghasemlou *et al*., 2011; Chen *et al*., 2010).

Al exhibited very high values of WVP_c (46.9 g·mm/d·m^2·kPa), which means that the film allowed the diffusion of high amounts of water vapor. High WVP_c is commonly found in films made from hydrogels or soluble polysaccharides as *Aloe* and gellan gum. For instance, mesquite gum films with a thickness of 152 μm reach a WVP of 59.31 g·mm/d·m^2·kPa (Bosquez-Molina *et al*., 2003) or alginate films (49 μm) a WVP of 146.8 g·mm/d·m^2·kPa (Olivas and Barbosa-Cánovas, 2008).

WVPc for Ge sample was 16.8 g·mm/d·m^2·kPa, that is 23.8 % less than Al. The low WVPc values of Ge can be explained based on the double-helix conformation of the gellan gum which creates a complex structure that moderately restricts the free permeation of water vapor (Takahashi *et al*., 2004). Some authors have reported several WVP values for gellan films and coatings in ranges of 315.3 to 422.4 and 21.84 to 34.32 with variable thickness of 170 to 178 μm and 80 to 90 μm, respectively (Tapia *et al*., 2008; Yang 1997). Yang *et al*., (2010) reported WVP values for gellan films treated with calcium from 7.2 to 30.96 g·mm/d·m^2·kPa and 30 μm to 65 μm, respectively, this report coincide with WVPc value of Ge obtained in the present work.

While, AlGe WVPc value was around 21.3 g·mm/d·m^2·kPa; *WVPc* values of Ge and AlGe had not significant difference ($P > 0.05$); this fact indicated an improvement of WVPc that is achieved when *Aloe vera* gel was mixed with gellan. The low value of *WVPc* found for AlGe could be explained by chemical interactions between mannans of *Aloe vera* and D-glucuronic acid of gellan gum that could create a self-crosslinked structure in the polysaccharides blend (Dentini *et al*., 2001), which diminishes the water vapor flux into the film. Microstructural evidence of the polysaccharides crosslinking can be seen in the AFM results (Fig. 7). Comparing with other protein-based films AlGe has minimal WVPc; for example, films from wheat gluten, corn zein and pistachio globulin had WVP values from 95.9 to 48.3, from 32.8 to 50.9, and from 55.4 to 96.2 g·mm/d·m^2·kPa, respectively (Park *et al*., 1994; Zahedi *et al*., 2010). In this regard, Mikkonen *et al*., (2010) also reported that the galactoglucomannans-based films had lower WVP (26 g·mm/d·m^2·kPa and thickness around 40 μm).

3.4 Nanomechanical properties

Fig. 9 shows the curves obtained by the nanoindenter, the three films showed different load-depth curves and Table 1 provides the Hd and Em values estimated for edible films. The Ge reached the maximum force at short displacement and Hd and Em values were high (171.9 MPa and 2.02 GPa, respectively) in comparison with Al and AlGe. The lack of glycerol in the Ge created a hard film, for that reason high Hd and Em values were obtained; therefore, Ge was not elastic and cracked easily. The Hd values found for Ge were similar to those reported for chitosan films (119-180 MPa) without glycerol (Wang *et al*., 2005; Lavorgna *et al*., 2010).

With respect to Al, the Berkovich indenter showed a deeper penetration into the film to reach the maximum load as compared to the other samples, consequently the load pause was larger and the unloading curve was more inclined. Therefore the Hd decreased to values around 0.9 MPa and the Em diminishes to 0.05 GPa, thus, Al can be describe as a soft and highly flexible film. The nanoindentation curve for AlGe was similar to Al, however the maximum force was reached with less displacement; the load pause was shorter than the one in Al and the load and unload curves had a less acute angle than the Al. The blend of the two polymers in AlGe enhances its nanomechanical properties with regard to the Al in around 40 % for Hd and in around 50% for Em. Nanoindentation technique allows to measure mechanical properties at nanometric levels, thus can be suggested that the reinforcement of these properties in AlGe could be attributed to a polysaccharides nanonetwork with cross-links on the films (Vachon *et al*., 2003; Del-Valle *et al*., 2005). Arzate-Vazquez (2011) fabricated alginate/chitosan films and found by nanoindentation technique, Hd and Em values around

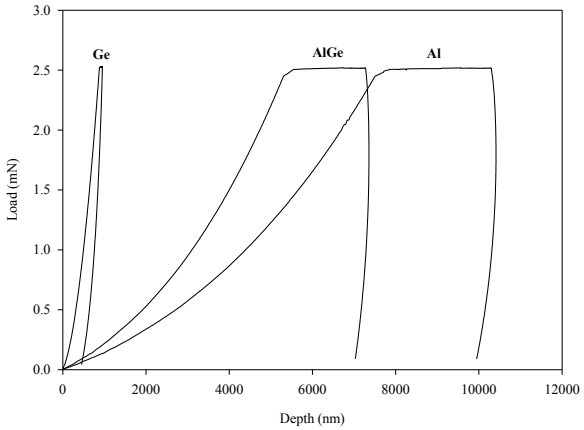

Fig. 9. Nanoindentation curves of films as a function of load and depth. *Aloe vera* film (Al); *Aloe vera* /gellan gum blend (AlGe) and gellan gum film (Ge). Each curve is an average of 5 indentations performed on three samples of each type of film.

16.2 MPa and 0.21 GPa; in contrast, AlGe was less hard (2.3 MPa) and more elastic (0.1 GPa).

Conclusions

Al, Ge and AlGe showed acceptable optical properties to be used as edible films, due to their values are similar to those edible films reported in other works. AlGe showed a major opacity and a higher difference in color. However, AlGe has an adequate appearance for its use in food industry. Also AlGe acquired the optical characteristics of the pure components, presenting intermediate gloss and *n* values in comparison with Al and Ge; maybe due to chemical interactions of *Aloe vera* and gellan gum.

Microstructural studies and image analysis were successful for evaluating the complexity, homogeneity and roughness of films. Furthermore, microscopy images were useful to evaluate the microstructural changes due to blending effect of pure components and drying process. AFM observations provided structural evidences of crosslinking between the polysaccharides of *Aloe vera* and gellan gum.

Chemical and structural interactions occurring in AlGe improved its functional properties, conferring some water impermeability in comparison with Al and water vapor transmission rates similar to those obtained for Ge. Additionally, the nanomechanical properties of AlGe were enhanced with respect to Al and Ge. Thus, the actual work could be a guide to design and characterize pure and blended edible films with novel functional properties.

Acknowledgements

Javier Segundo Alvarado-González wishes to thank CONACyT for the scholarship provided. This research was financial through the projects, 20110627, 20121001 at the Instituto Politécnico Nacional (SIP-IPN-Mexico), 133102 (CONACyT) and Cátedra Coca-Cola para jóvenes investigadores 2011 (Coca Cola-CONACYT). The authors also wish to thank the Centro de Nanociencias y Micro y Nanotecnologías (CNMN) IPN and Instituto Mexicano del Petróleo.

References

Abugoch, L.E., Tapia, C., Villamán, M.C., Yazdani-Pedram, M. and Díaz-Dosque, M. (2011). Characterization of quinoa protein-chitosan blend edible films. *Food Hydrocolloids 25*, 879-886.

Adachi, N. (2002). Dehydrated gel composition from hydrated isolated acetylated gellan gum. *Patent: US006458404B1*. United States Patent.

Alves, P.M.A., Carvalho, R.A., Moraes, I.C.F., Luciano, C.G., Bittante, A.M.Q.B. and Sobral, P.J.A. (2011). Development of films based on blends of gelatin and poly(vinyl alcohol) cross linked with glutaraldehyde. *Food Hydrocolloids Volume 25*, 1751-1757.

Arzate-Vazquez, I. (2011). *Aplicación del análisis de textura de imágenes para la caracterización cuantitativa de superficies biológicas*. Tesis de doctorado en alimentos. Escuela Nacional de Ciencias Biológicas del Instituto Politécnico Nacional.

Arzate-Vázquez, I., Chanona-Pérez, J.J., Calderón-Domínguez, G., Terres-Rojas, E., Garibay-Febles, V., Martínez-Rivas, A. and Gutiérrez-López, G.F. (2012). Microstructural characterization of chitosan and alginate films by microscopy techniques and texture image analysis. *Carbohydrate Polymers 87*, 289-299.

ASTM. (1989). Standard test methods for water vapor transmission of materials E 96-80. In *Annual book of ASTM standards* (pp. 745-754). Philadelphia, PA: American Society for Testing and Materials.

ASTM. (1999). Standard test method for specular gloss. In Designation (D523). *Annual book of ASTM standards*, Vol. 06.01. Philadelphia, PA: American Society for Testing and Materials.

ASTM. (2000c). Standard Test Method for Transparency of Plastic Sheeting. Designation D1746-97, vol. 8.01. American Society for Testing and Materials, Philadelphia, PA.

Ayranci, E. and Tunc, S. (2003). A method for the measurement of the oxygen permeability and the development of edible films to reduce the rate of oxidative reactions in fresh foods. *Food Chemistry 80*, 423-431.

Banerjee, S. and Bhattacharya, S. (2011). Compressive texture attributes, opacity and syneresis of gels prepared from gellan, agar and their mixtures. *Journal of Food Engineering 102*, 287-292.

Barkalow, D.G., Chapdelaine, A.H. and Dzija, M.R. (2002). Pullulan free edible film compositions and methods of making the same. *Patent: US 20020131990A1*. United States Patent.

Bergo, P., Sobral, P.J.A. and Prison, J.M. (2010). Effect of glycerol on physical properties of cassava starch films. *Journal of Food Processing and Preservation 34*, 401-410.

Bósquez-Molina, E., Guerrero-Legarreta, I. and Vernon-Carter, E.J. (2003). Moisture barrier properties and morphology of mesquite gum-candelilla wax based edible emulsion coatings. *Food Research International 36*, 885-893.

Carneiro-da-Cunha, M.G., Cerqueira, M.A., Souza, B.W.S., Carvalho, S., Quintas, M.A.C., Teixeira, J.A. and Vicente, A.A. (2010). Physical and thermal properties of a chitosan/alginate nanolayered PET film. *Carbohydrate Polymers 82*, 153-159.

Castillo, S., Navarro, D., Zapata, P.J., Guillén, F., Valero, D., Serrano, M. and Martínez-Romero, D. (2010) Antifungal efficacy of *Aloe vera* in vitro and its use as a preharvest treatment to maintain postharvest table grape quality. *Postharvest Biology and Technology 57*, 183-188.

Çaykara, T. (2004). Effect of maleic acid content on network structure and swelling properties of poly(N-isopropylacrylamide-co-maleic acid) polyelectrolyte hydrogels. *Journal of Applied Polymer Science 92*, 763-769.

Çaykara, T. and Turan, E. (2006). Effect of the amount and type of the crosslinker on the swelling behavior of temperature-sensitive poly(N-tert-butylacrylamide-co-acrylamide) hydrogels. *Colloid and Polymer Science 284*, 1038-1048.

Chen, C.-P., Wang, B.-J. and Weng, Y.-M. (2010). Physiochemical and antimicrobial properties of edible aloe/gelatin composite films. *International Journal of Food Science & Technology 45*, 1541-1544.

Del-Valle, V., Hernández-Muñoz, P., Guarda, A. and Galotto, M.J. (2005). Development of a cactus-mucilage edible coating (*Opuntia ficus indica*) and its application to extend strawberry (*Fragaria ananassa*) shelf-life. *Food Chemistry 91*, 751-756.

Dentini, M., Desideri, P., Crescenzi, V., Yuguchi, Y., Urakawa, H. and Kajiwara, K. (2001). Synthesis and physicochemical characterization of gellan gels. *Macromolecules 34*, 1449-1453.

Domínguez-Fernández, R.N., Arzate-Vázquez, I., Chanona-Pérez, J.J, Welti-Chanes, J.S., Alvarado-González, J.S., Calderón-Domínguez, G., Garibay-Febles, V. and Gutiérrez-López, G.F. (2012). El gel de *Aloe vera*: Estructura, composición química, procesamiento, actividad biológica e importancia en la industria farmacéutica y alimentaria. *Revista Mexicana de Ingeniería Química 11*, 23-43.

Fabra, M.J., Hambleton, A., Talens, P., Debeaufort, F. and Chiralt, A. (2011). Effect of ferulic acid and α-tocopherol antioxidants on properties of sodium caseinate edible films. *Food Hydrocolloids 25*, 1441-1447.

Femenia, A., García-Pascual, P., Simal, S. and Rosellò, C. (2003). Effects of heat treatment and dehydration on bioactive polysaccharide acemannan and cell wall polymers from *Aloe barbadensis* Miller. *Carbohydrate Polymers 51*, 397-405.

Fernández-Pan, I., Ziani, K., Pedroza-Islas, R. and Maté, J.I. (2010). Effect of drying conditions on the mechanical and barrier properties of films

based on chitosan. *Drying Technology 28*, 1350-1358.

Fischer-Cripps, A.C. (2006). Critical review of analysis and interpretation of nanoindentation test data. *Surface & Coating Technology 200*, 4153-4165.

Funami,T., Noda, S., Nakauma, M., Ishihara, S., Takahashi, R., Al-Assaf, S., Ikeda, S., Nishinari, K. and Phillips, G.O. (2008) Molecular structures of gellan gum imaged with atomic force microscopy in relation to the rheological behavior in aqueous systems in the presence or absence of various cations. *Journal of Agricultural and Food Chemistry 56*, 8609-8618.

Gennadios, A., Weller, C.L. and Gooding, C.H. (1994). Measurement errors in water vapor permeability of highly permeable, hydrophilic edible films. *Journal of Food Engineering 21*, 395-409.

Ghasemlou, M., Khodaiyan, F. and Oromiehie, A. (2011). Physical, mechanical, barrier, and thermal properties of polyol-plasticized biodegradable edible film made from kefiran. *Carbohydrate Polymers 84*, 477-483.

Hans, J.H. and Floros, J.D. (1997). Casting antimicrobial packaging films and measuring their physical properties and antimicrobial activity. *Journal of Plastic Film & Sheeting 13*, 287-98.

Haralick, R. M., Shanmugam, K., and Dinstein, I. (1973). Textural features for image classification. *IEEE Transactions on Systems, Man and Cybernetics SMC 3*, 610-621.

Ikoni, O. and Obiageli, N. (2010). Film coating potential of okra gum using paracetamol tablets as a model drug. *Asian Journal of Pharmaceutics 4*, 130-134.

Illiger, S.R., Fadnis, C., Demappa, T., Jayaraju, J. and Keshavayya, J. (2009). Miscibility studies of HPMC/PEG blends in water by viscosity, density, refractive index and ultrasonic velocity method. *Carbohydrate Polymers 75*, 484-488.

Jones, J.B. (2010). *Physical characteristics and metal binding applications of chitosan films*. Master's Thesis. University of Tennessee. http://trace.tennessee.edu/utk_gradthes/722

Jung, C.H. and Kim, Y.P. (2008). Theoretical study on the change of the particle extinction coefficient during the aerosol dynamic processes. *Journal of Aerosol Science 39*, 904-916.

Jutaporn, C.T., Suphitchaya, C. and Thawien, W. (2011). Antimicrobial activity and characteristics of edible films incorporated with Phayom wood (*Shorea tolura*) extract. *International Food Research Journal 18*, 39-54.

Kechichian, V., Ditchfield, C., Veiga-Santos, P. and Tadini, C.C. (2010). Natural antimicrobial ingredients incorporated in biodegradable films based on cassava starch. *LWT Food Science and Technology 43*, 1088-1094.

Krumova, M., Flores, A., Baltá Calleja, F.J. and Fakirov, S. (2002). Elastic properties of oriented polymers, blends and reinforced composites using the microindentation technique. *Colloid & Polymer Science 280*, 591-598.

Lau, M.H., Tang, J. and Paulson, A.T. (2001). Effect of polymer ratio and calcium concentration on gelation properties of gellan/gelatin mixed gels. *Food Research International 34*, 879-886.

Lavorgna, M., Piscitelli, F., Mangiacapra, P. and Buonocore, G.G. (2010). Study of the combined effect of both clay and glycerol plasticizer on the properties of chitosan films. *Carbohydrate Polymers 82*, 291-298.

Lee, K.Y., Shim, J. and Lee, H.G. (2004) Mechanical properties of gellan and gelatin composite films. *Carbohydrate Polymers 56*, 251-254.

Lee, J.-W., Son, S.-M. and Hong, S.-I. (2008). Characterization of protein-coated polypropylene films as a novel composite structure for active food packaging application. *Journal of Food Engineering 86*, 484-493.

Liu, Z., Ge, X., Lu, Y., Dong, S., Zhao, Y. and Zeng, M. (2012). Effects of chitosan molecular weight and degree of deacetylation on the properties of gelatine-based films. *Food Hydrocolloids 26*, 311-317.

Liu, J.-G., Nakamura, Y., Shibasaki, Y., Ando, S. and Ueda, M. (2007). High refractive index polyimides derived from 2,7-bis(4-aminophenylenesulfanyl)thianthrene and

aromatic dianhydrides. *Macromolecules 40*, 4614-4620.

Lucca, D.A., Herrmann, K. and Klopfstein, M.J. (2010). Nanoindentation: Measuring methods and applications. *CIRP Annals - Manufacturing Technology 59*, 803-819.

Maria, T.M.C., De Carvalho, R.A., Sobral, P.J.A., Habitante, A.M.B.Q. and Solorza-Feria, J. (2008). The effect of the degree of hydrolysis of the PVA and the plasticizer concentration on the color, opacity, and thermal and mechanical properties of films based on PVA and gelatin blends. *Journal of Food Engineering 87*, 191-199.

Mendoza, F., Dejmek, P. and Aguilera, J. M. (2007). Colour and image texture analysis in classification of commercial potato chips. *Food Research International 40*, 1146-1154.

Meraz-Torres, L.S., Quintanilla-Carvajal, M.X., Hernández-Sánchez, H., Téllez-Medina, D.I., Alamilla-Beltrán, L. and Gutierrez-López, G.F. (2011). Assessment of the kinetics of contact angle during the wetting of maltodextrin agglomerates. *Revista Mexicana de Ingeniería Química 10*, 273-279.

Mikkonen K.S., Heikkilä M.I., Helén H., Hyvönen L. and Tenkanen M. (2010). Spruce galactoglucomannan films show promising barrier properties. *Carbohydrate Polymers 79*, 1107-1112.

Miranda, M., Vega-Gávez, A., García, P., Di Scalad, K., Shi, J., Xue, S. and Uribe, E. (2010). Effect of temperature on structural properties of *Aloe vera* (*Aloe barbadensis* Miller) gel and Weibull distribution for modelling drying process. *Food and Bioproducts Processing 88*, 138-144.

Miyoshi, E. (2007). Different effects of monosaccharides and disaccharides on the sol-gel transition in gellan gum aqueous solutions. *Development and Environment 7*, 31-43.

Monedero, F.M., Fabra, M.J., Talens, P. and Chiralt, A. (2008). Effect of oleic acid-beeswax mixtures on mechanical, optical and water barrier properties of soy protein isolate based films. *Journal of Food Engineering 91*, 509-515.

Montgomery, D. C. (1991). *Design and Analysis of Experiments*. Wiley & Sons, Inc. USA.

Moreira, L.R.S. and Filho, E.X.F. (2008). An overview of mannan structure and mannan-degrading enzyme systems. *Applied Microbiology Biotechnology 79*,165-178.

Mu, C., Guo, J., Li, X., Lin, W. and Li, D. (2012). Preparation and properties of dialdehyde carboxymethyl cellulose crosslinked gelatin edible films. *Food Hydrocolloids 27*, 22-29.

Murray, C.A. and Dutcher, J.R. (2006). Effect of changes in relative humidity and temperature on ultrathin chitosan films. *Biomacromolecules 7*, 3460-3465.

Nadarajah, K. (2005). *Development and characterization of antimicrobial edible films from crawfish chitosan*. Louisiana State University, Electronic Thesis & Dissertation Collection. URN etd-04142005-152845.

Nosal, W.H., Thompson, D.W., Yan, L., Sarkar, S., Subramanian, A. and Woollam, J.A. (2005). UV-vis-infrared optical and AFM study of spin-cast chitosan films. *Colloids and Surfaces B: Biointerfaces 43*, 131-137.

Oakenfull, D.G. (1991). The chemistry of high-methoxyl pectins. In R.H. Walter (Ed.) *The chemistry and technology of pectins* (pp. 87-108). New-York: Academic Press.

Olivas, G.I. and Barbosa-Cánovas, G.V. (2008). Alginate-calcium films: Water vapor permeability and mechanical properties as affected by plasticizer and relative humidity. *LWT- Food Science and Technology 41*, 359-366.

Oliver, W.C. and Pharr, G.M. (2004). Measurement of hardness and elastic modulus by instrumented indentation: Advances in understanding and refinements to methodology. *Journal of Materials Research 19*, 3-20.

Padmakumari. P., Anupama, C., Abbulu, K.and Pratyusha, A.P. (2011). Evaluation of fruit calyces mucilage of Hibiscus Sabdariffa Linn as tablet binder. *International Journal of Research in Pharmaceutical and Biomedical Sciences 2*, 516-519.

Park, H.J., Bunn, J.M., Weller, C.L., Vergano, P.J. and Testin, R.F. (1994). Water vapor permeability and mechanical properties of grain protein-based films as affected by mixtures of polyethylene glycol and glycerin plasticizers. *Transactions of the American Society of Agricultural Engineers 37*, 1281-1285.

Piña, Z.H.J. and Morales, E.A. (2010). Aloe en Venezuela: de la cadena de valor al distrito industrial. *Problemas del Desarrollo: Revista Latinoamericana de Economía 41*, 187-208.

Porter, S.C. and Felton, L.A. (2010). Techniques to assess film coatings and evaluate film-coated products. *Drug Development and Industrial Pharmacy 36*, 128-142.

Pranoto, Y., Lee, C.M. and Park, H.J. (2007). Characterizations of fish gelatin films added with gellan and κ-carrageenan. *LWT - Food Science and Technology 40*, 766-774.

Quintanilla-Carvajal, M.X., Meraz-Torres, L.S., Alamilla-Beltrán, L., Chanona-Pérez, J.J., Terres-Rojas, E., Hernández-Sánchez, H., Jiménez-Aparicio, A.R. and Gutierrez-López, G.F. (2011). Morphometric characterization of spray-dried microcapsules before and after α-tocopherol extraction. *Revista Mexicana de Ingeniería Química 10*, 301-312.

Ramachandra, C.T. and Srinivasa Rao, P. (2008). Processing of *Aloe vera* leaf gel: A review. *American Journal of Agricultural and Biological Sciences 3*, 502-510.

Ramachandra, C.T. and Srinivasa Rao, P. (2009). Modelling and optimization of drying variables in desiccant air drying of *Aloe vera* (*Aloe barbadensis* Miller) gel. *ASABE 2009 Reno, Nevada, 096498*.

Rodríguez-González, V.M., A. Femenia, A., Minjares-Fuentes, R. and González-Laredo, F. R. (2012) Functional properties of pasteurized samples of Aloe barbadensis Miller: Optimization using response surface methodology. *LWT - Food Science and Technology 47*, 225-232

Rojas-Graü, M.A., Tapia, M.S. and Martín-Belloso, O. (2008). Using polysaccharide-based edible coatings to maintain quality of fresh-cut Fuji apples. *LWT-Food Science and Technology 41*, 139-147.

Romero-Bastida, C.A., Zamudio-Flores P.B. and Bello-Perez L.A. (2011). Antimicrobianos en películas de almidón oxidado de plátano: efecto sobre la actividad antibacteriana, microestructura, propiedades mecánicas y de barrera. *Revista Mexicana de Ingeniería Química 10*, 445-453.

Saibuatong, O. and Phisalaphong, M. (2010). Novo aloe vera-bacterial cellulose composite film from biosynthesis. *Carbohydrate Polymers 79*, 455-460.

Sittikijyothin, W., Torres, D. and Gonçalves, M.P. (2005). Modelling the rheological behaviour of galactomannan aqueous solutions. *Carbohydrate Polymers 59*, 339-350.

Takahashi, R., Tokunou, H., Kubota, K., Ogawa, E., Oida, T., Kawase, T. and Nishinari, K. (2004). Solution properties of gellan gum: change in chain stiffness between single- and double-stranded chains. *Biomacromolecules 5*, 516-523.

Tang, J., Tung, M.A. and Zeng, Y. (1998). Characterization of gellan gels using stress relaxation. *Journal of Food Engineering 38*, 279-295.

Tapia, M.S., Rojas-Graü, M.A., Carmona, A., Rodriguez, F.J., Soliva-Fortuny, R. and Martin-Belloso, O. (2008). Use of alginate- and gellan-based coatings for improving barrier, texture and nutritional properties of fresh-cut papaya. *Food Hydrocolloids 22*, 1493-1503.

Vachon, C., D'aprano, G., Lacroix, M. and Letendre, M. (2003). Effect of edible coating process and irradiation treatment of strawberry fragaria spp. on storage-keeping quality. *Journal of Food Science 68*, 608-612.

Villagómez-Zavala, D.L., Gómez-Corona, C., San Martín Martínez, E., Pérez-Orozco, J.P., Vernon-Carter, E.J. and Pedroza-Islas, R. (2008). Comparative study of the mechanical properties of edible films made from single and blended hydrophilic biopolymer matrices. *Revista Mexicana de Ingeniería Química 7*, 263-273.

Villalobos, R., Chanona, J., Hernández, P., Gutiérrez, G. and Chiralt, A. (2005). Gloss and transparency of hydroxypropyl methycellulose

films containing surfactants as affected by their microstructure. *Food Hydrocolloids 19*, 53-61.

Wang, S.-F., Shen, L., Zhang, W.-D. and Tong, Y.J. (2005). Preparation and mechanical properties of chitosan/carbon nanotubes composites. *Biomacromolecules 6*, 3067-3072.

Wang, Y., Li, D., Wang, L., Yang, L. and Ózkan, N. (2011) Dynamic mechanical properties of flaxseed gum based edible films. *Carbohydrate Polymers 86*, 499-504.

Ward, G. and Nussinovitch, A. (1997). Characterizing the gloss properties of hydrocolloid films. *Food Hydrocolloids 11*, 357-365.

Wei, P.-J. and Lin, J.-F. (2005). A new method developed to evaluate both the hardness and elastic modulus of a coating-substrate system. *Surface & Coatings Technology 200*, 2489-2496.

Yang, L. (1997). *Physicochemical properties of biodegradable/edible films made with gellan gum*. Technical University of Nova Scotia, Electronic Thesis & Dissertation Collection. Id.: 50989058

Yang, X., Beyenal, H., Harkin, G., and Lewandowski, Z. (2000). Quantifying biofilm structure using image analysis. *Journal of Microbiological Methods 39*, 109-119.

Yang, H., Wang, Y., Lai, S., An, H., Li, Y. and Chen, F. (2007). Application of atomic force microscopy as a nanotechnology tool in food science. *Journal of Food Science 72*, R65-R75.

Yang, L., Paulson, A.T. and Nickerson, M.T. (2010). Mechanical and physical properties of calcium-treated gellan films. *Food Research International 43*, 1439-1443.

Yener, F.Y.G., Korel, F. and Yemenicioglu, A. (2009). Antimicrobial activity of lactoperoxidase system incorporated into cross-linked alginate films. *Journal of Food Science 74*, M73-M79.

Zahedi, Y., Ghanbarzadeh, B. and Sedaghat, N. (2010). Physical properties of edible emulsified films based on pistachio globulin protein and fatty acids. *Journal of Food Engineering 100*, 102-108.

Zhang, S. and Zhang, X. (2012). Toughness evaluation of hard coatings and thin films: A critical review. *Thin Solid Films 520*, 2375-2389.